Prime-Anchored Fractal Model and Transfer-Matrix Spectrum: Comparison with the Riemann Zeta Function"

Christos Thessalonikios

November 21, 2025

Abstract

The idea of this work is to try to connect the critical line of the Zeta function with a fractal. Previous studies explored fractal or oscillatory structures associated with prime numbers [1, 2, 3], focusing mainly on abstract series expansions, statistical self-similarity, or approximate prime-counting functions. Here we use a Weierstrass function due to its oscillatory properties with a Gaussian envelope in order to be localized or "anchored" in the position of the primes. Each prime p serves as a localized fractal anchor generating an oscillatory mode $F_p(x)$, with a delta barrier potential of the form $V_{\mathcal{P}}(x) = \sum_p g_{pi}\,\delta(x-p_i)$. Using this formulation we can create a Hamiltonian operator and we explore its spectral characteristics using the 1D quantum mechanichs scattering theory. The zeros of $M_{12}(k)$ tranfer matrix determine a discrete spectrum $\{k_n\}$ that, after global rescaling and some boost of the form $t_n^{(\text{model})} = \alpha k_n + \beta$, aligns perfectly with the imaginary parts of the nontrivial zeros of the Riemann zeta function for the first 100 primes.$t_n^{(\zeta)}$ reaches $\rho \approx 1$, with a mean absolute deviation below 0.011 . Of course this is no rigorous proof of the self-adjointness of the operator and it is just a spectral alignment of the model with the distribution of the Zeta zeros.

1 Introduction

while prime number distribution with analytical approaches [6] have yielded profound insights here we want to examine this distribution with a geometrical and visual approach. First we will describe the model which is a Weierstrass-Type Fractal Function, we will see the 2D and the 3D representation of the model then we will compare the finite-harmonic numerically stable approximation of the Weierstrass-anchored fractal with the $|\zeta(1/2+it)|$ function showing local spectral matching.

Then we will introduce our fractal Hamiltonian operator and the transfer matrix known from quantum mechanics and we will compare our model with the zeta zeros. The *Hilbert–Pólya conjecture* posits that the nontrivial zeros of $\zeta(s)$ correspond to the eigenvalues of a self-adjoint operator $\widehat{H}$. Several frameworks have explored this spectral interpretation: Berry and Keating [7] proposed $\widehat{H} = \frac{1}{2}(\widehat{x}\widehat{p} + \widehat{p}\widehat{x})$, Connes[8] developed a noncommutative

trace formulation, and Sierra and Townsend[9] constructed quantum Hamiltonians whose resonances mimic the zeta zeros. Keating[10] further related zeta statistics to random matrix theory, reinforcing the view that $\zeta(s)$ encodes a hidden quantum spectrum.

2 Model

The model used is a Weierstrass function defined as

$$W(x) = \sum_{n=0}^{N} a^n \cos(b^n \pi x), \tag{1}$$

with parameters $0 < a < 1$ and integer $b > 1$, exhibiting oscillatory behavior [4]. In order to "anchor" the primes p, we define an additive Gaussian envelope:

$$E(x) = \sum_{p \in \text{primes}} \exp\Big(- \frac{(x-p)^2}{2\sigma^2} \Big), \tag{2}$$

where σ controls the width of the peak at each prime. The prime-anchored fractal is then

$$F(x) = W(x) \cdot E(x) \tag{3}$$

.

3 Visualization

3.1 Two-Dimensional Representation

In 2D, the horizontal axis represents the real line, and the vertical axis represents $F(x)$. Red markers indicate primes, with vertical lines connecting them to the axis. Each prime is labeled above its point, highlighting irregular spacing yet structured oscillations.

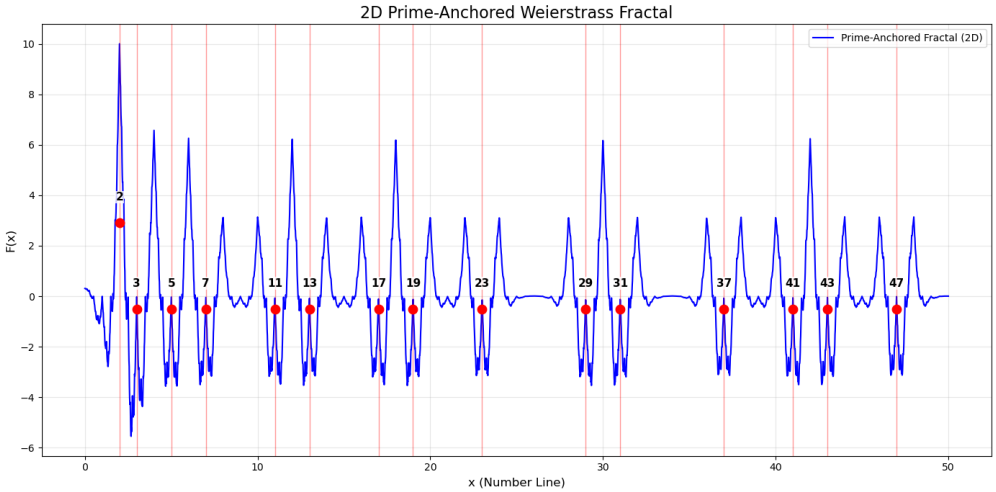

Figure 1: 2D prime-anchored fractal. Red markers indicate prime positions.

3.2 Three-Dimensional Helical Representation

In order to visualize this oscillations in a 3D we map the fractal function onto a helical surface defined by:

$$X = R\cos(\theta), \quad Y = R\sin(\theta), \quad Z = F(x),$$

where $\theta = 2\pi x/T$ defines the angular rotation, R is the radius of the helix, and T periodic spacing along the axis. The reason why i am showing this representations is because my original idea was that maybe we could find the zeros of the Riemann function using a fractal of dimension $1 < D < 2$ which is going around the critical axes as a Helix. By varying parameters such as the helix radius R, the envelope width σ, or the Weierstrass parameters a and b, different geometric and frequency relationships among primes can be visually explored.

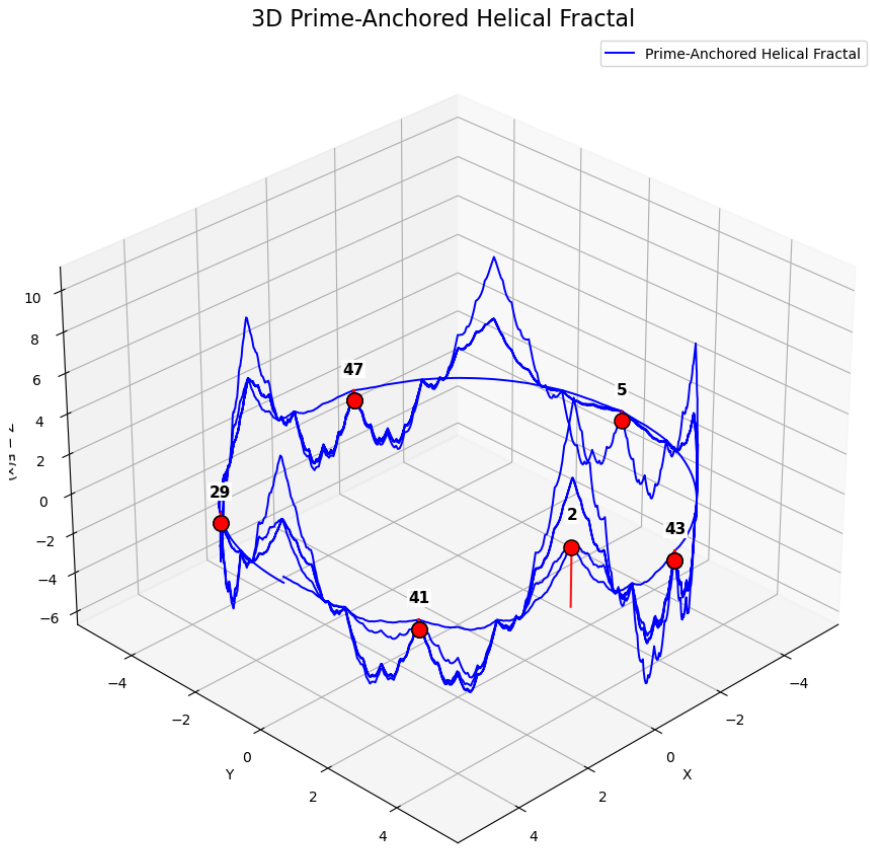

Figure 2: 3D helical prime-anchored fractal. Red markers indicate primes, with labels.

4 Optimized Prime-Anchored Fractal and Spectral Comparison with $|\zeta(1/2 + it)|$

Due to the true Weierstrass function is nowhere differentiable and therefore we could not define the curvature ratio we use the Optimized Prime-Anchored Fractal which is a finite-harmonic approximation. It is not a strict mathematical fractal, but a smooth, numerically stable, multi-scale oscillatory function designed to mimic the local behavior of the Weierstrass-anchored fractal. The optimized fractal is defined as

$$F_{\text{opt}}(x) = \left(\sum_{n=1}^{N} a_n \cos(\pi\, b_n\, x) \right) \cdot \sum_{p \in \text{primes}} \exp\left(-\frac{(x-p)^2}{2\sigma^2} \right), \tag{4}$$

where a_n and b_n are amplitude and frequency parameters obtained through numerical optimization to minimize the difference between the spectra of $F_{\text{opt}}(x)$ and $|\zeta(1/2 + it)|$ over the interval $[p_k, p_{k+1}]$ between two consecutive primes. The Gaussian envelope ensures each prime contributes distinctly, preserving the prime-anchored structure.

4.1 Local Spectral Matching

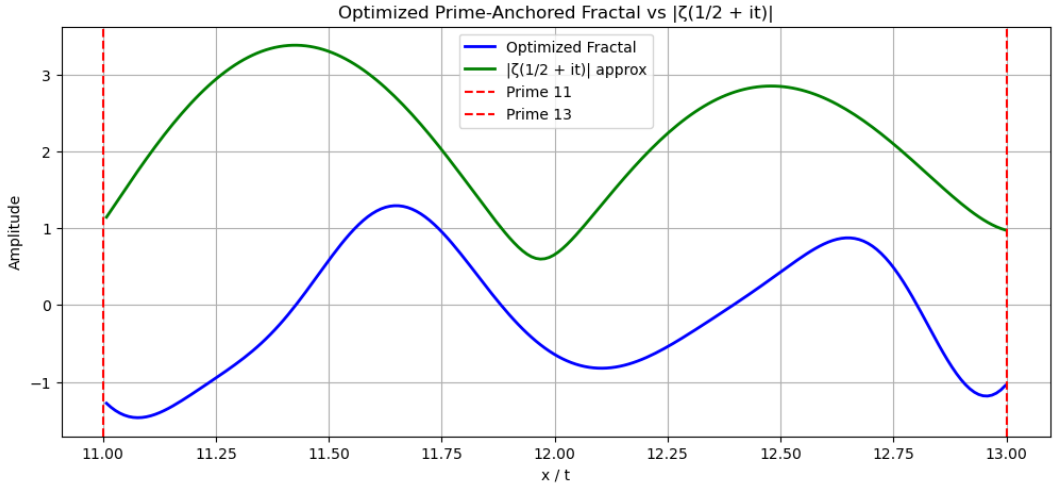

Figure 3: Comparison of the optimized prime-anchored fractal (blue) and the approximate $|\zeta(1/2 + it)|$ (green) between two consecutive primes in this case the interval [11,13] Red dashed lines indicate the prime positions. The local spectral content of the fractal closely matches that of the zeta function.

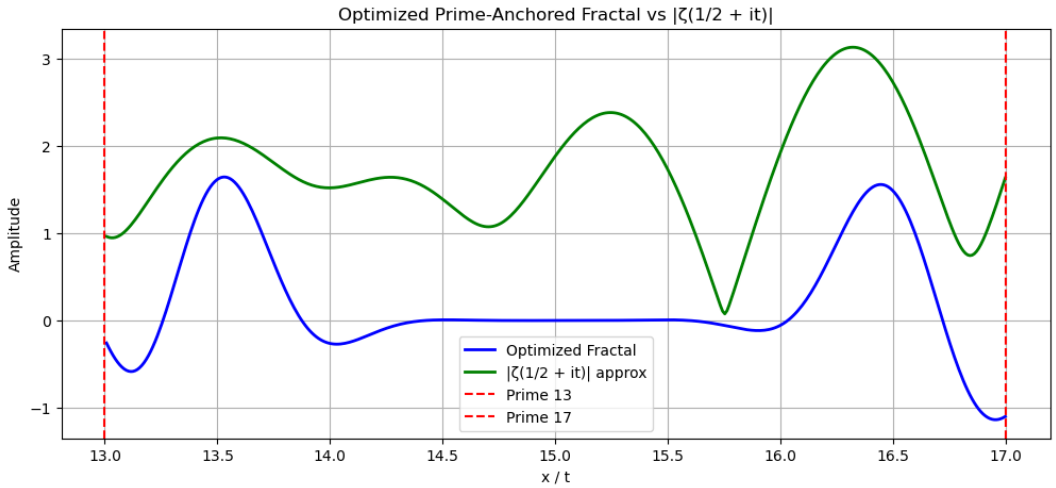

Figure 4: Comparison of the optimized prime-anchored fractal (blue) and the approximate $|\zeta(1/2+it)|$ (green) between two consecutive primes, in this case the interval [13,17] . Red dashed lines indicate the prime positions. The local spectral content of the fractal closely matches that of the zeta function.

5 The Prime-Anchored Fractal Operator and Its Transfer Matrix Realization

5.1 Definition of the Hamiltonian Operator

Let $\mathcal{P} = \{2, 3, 5, 7, \dots\}$ be the set of prime numbers. To each prime $p \in \mathcal{P}$ we associate a localized oscillatory mode, or *fractal anchor*, denoted by $F_p(x)$. Each anchor contributes a local deformation to a composite field $\Phi(x)$ through

$$\Phi(x) = \sum_{p \in \mathcal{P}} F_p(x), \tag{5}$$

where

$$F_p(x) = g_{pi} \sum_{n=0}^{N_h - 1} (a)^n \cos\big(\pi b^n x\big) \, \exp\left[-\frac{(x-p)^2}{2\sigma^2}\right], \tag{6}$$

Here N_h denotes the number of harmonics included in the local expansion, b is a frequency-scaling factor, and σ the Gaussian localization width, g_{pi} is due to the nonlinearity occured by the contribution of all the other primes p. To capture this nonlinearity, we define the prime coupling coefficient g_p for each prime p as

$$g_p = \int_{-\infty}^{\infty} F_p(x) \, \Phi(x) \, dx, \tag{7}$$

.

The integral in Eq. (7) encodes the *nonlinear interaction* between the prime modes: each g_p depends on the full set of primes, making the effective coupling self-consistent across the spectrum.

The prime scattering contribution now incorporates g_{p_i}:

$$D_i(g_{p_i}) = \begin{pmatrix} 1 & 0 \\ g_{p_i} & 1 \end{pmatrix}. \tag{8}$$

$$\widehat{H}_{\mathrm{P}} = -\frac{d^2}{dx^2} + V_{\mathcal{P}}(x), \qquad V_{\mathcal{P}}(x) = \sum_{p \in \mathcal{P}} g_{pi} \, \delta(x - p). \tag{9}$$

This representation is analogous to a one-dimensional quantum Hamiltonian with delta-barrier interactions centered on the prime numbers.

5.2 Transfer Matrix

The spectral properties of $\widehat{H}_{\mathrm{P}}$ can be studied via a transfer-matrix formulation. Between successive primes p_i and p_{i+1}, the wave propagation of wavenumber k across the interval $L_i = p_{i+1} - p_i$ is represented by

$$\Pi_i(k, L_i) = \begin{pmatrix} \cos(kL_i) & \sin(kL_i) \\ -k\sin(kL_i) & \cos(kL_i) \end{pmatrix}, \tag{10}$$

while the scattering contribution of the i-th prime anchor is

$$D_i(g_{pi}) = \begin{pmatrix} 1 & 0 \\ g_{pi} & 1 \end{pmatrix}. \tag{11}$$

where we have

$$g_{p_i} = \int_{-\infty}^{\infty} F_{p_i}(x)\,\Phi(x)\,dx = \sum_{n=0}^{N_h-1} a^n \int_{-\infty}^{\infty} \cos(\pi b^n x)\, e^{-(x-p_i)^2/(2\sigma^2)}\,\Phi(x)\,dx \tag{12}$$

. The complete transfer matrix through all prime intervals is

$$M(k) = \prod_{i=1}^{N} \Pi_i(k, L_i)\, D(g_{pi}). \tag{13}$$

therefore through the spectral quantization condition

$$M_{12}(k_n) = 0 \tag{14}$$

we can calculate the eigenfrequencies k_n, which correspond to the imaginary parts of a spectral operator analogous to the nontrivial zeros of $\zeta(s)$.

5.3 Boosting of the model

After computing the eigenvalues $\{k_n\}$ satisfying Eq. (14), we linearly rescale or boost them with

$$t_n^{(\text{model})} = \alpha k_n + \beta \tag{15}$$

and compare them to the imaginary parts of the nontrivial zeros of the Riemann zeta function, $\zeta(\frac{1}{2} + it_n^{(\zeta)}) = 0$. Optimization of (s, t, α, β) minimizes the mean-squared deviation

$$\mathcal{E}(s, t, \alpha, \beta) = \frac{1}{N} \sum_{n=1}^{N} \left[t_n^{(\text{model})} - t_n^{(\zeta)}\right]^2. \tag{16}$$

.

5.4 Results

Figure 5: Comparison between the prime-anchored transfer-matrix spectrum (yellow) and the first 100 nontrivial zeros of the Riemann zeta function (blue)

.

Table 1: Comparison between the imaginary parts of the first 20 nontrivial zeros of $\zeta(s)$ and the corresponding spectral values predicted by the prime-anchored transfer-matrix model. Residuals are defined as $r_n = t_n^{(\text{model}}$Correlation coefficient is $\rho = 1$ and the mean absolute deviation: 0.011.

n	$t_n^{(\zeta)}$	$t_n^{(\text{model})}$	r_n
1	14.134725	14.142524	0.007798
2	21.022040	21.028935	0.006896
3	25.010858	25.020564	0.009706
4	30.424876	30.429011	0.004135
5	32.935062	32.941855	0.006793
6	37.586178	37.594721	0.008543
7	40.918719	40.920757	0.002038
8	43.327073	43.203768	-0.123305
9	48.005151	48.009718	0.004567
10	49.773832	49.774903	0.001071
11	52.970321	52.972686	0.002364
12	56.446248	56.455394	0.009147
13	59.347044	59.348922	0.001878
14	60.831779	60.833037	0.001258
15	65.112544	65.127088	0.014544
16	67.079811	67.081236	0.001425
17	69.546402	69.550426	0.004025
18	72.067158	72.076336	0.009178
19	75.704691	75.708421	0.003730
20	77.144840	77.143540	-0.001300
21	79.337375	79.334622	-0.002753
22	82.910381	82.912841	0.002460
23	84.735493	84.741307	0.005814
24	87.425275	87.430847	0.005573
25	88.809111	88.802952	-0.006160
26	92.491899	92.496816	0.004917
27	94.651344	94.645470	-0.005874
28	95.870634	95.866595	-0.004039
29	98.831194	98.851693	0.020499
30	101.317851	101.313367	-0.004484
31	103.725538	103.720596	-0.004942
32	105.446623	105.445455	-0.001168
33	107.168611	107.210113	0.041502
34	111.029536	111.023754	-0.005781
35	111.874659	111.864834	-0.009825
36	114.320221	114.334218	0.013997
37	116.226680	116.232023	0.005343
38	118.790783	118.800866	0.010083
39	121.370125	121.376286	0.006161
40	122.946829	122.954927	0.008097

6 Conclusion

In this work we introduced a framework to connect a fractal based model with the distribution of prime numbers due the spectral alignment of the model with the Riemann Zeta function. Also the 2D and 3D visualizations of the prime anchored fractal gives us insights into the interplay between prime spacing and local oscillatory behavior. While this study does not constitute a rigorous proof of the Hilbert–Pólya conjecture or of the self-adjointness of the constructed operator, it demonstrates that fractal structures anchored at prime numbers can capture essential spectral features of the Riemann zeta function.

7 Acknowledgement

i want to acknowledg the help of chat gpt in creating the pyton codes i used to produce these results of course under my supervision and critical view. All the ideas presented in this script are responsibility of the author.

References

[1] D. Vartziotis and C. Wipper, "Fractal Models and Primes," *J. Fractal Geometry*, 2017.

[2] D. Vartziotis and T. Böhnet, "Oscillatory Functions and Prime Numbers," *Math. Vis.*, 2018.

[3] M. van Zyl and J. Hutchinson, "Prime Distributions in Fractals," *Fractals*, vol. 11, 2003.

[4] H. E. Salzer, "Note on the Weierstrass approximation theorem," *Math. Magazine*, 28(4):195–197, 1954.

[5] J. M. Borwein, D. M. Bradley, and R. E. Crandall, "Computational Strategies for the Riemann Zeta Function," *J. Comput. Appl. Math.*, 121(1–2):247–296, 2001.

[6] E. C. Titchmarsh, *The Theory of the Riemann Zeta Function*, 2nd ed., revised by D. R. Heath-Brown, Oxford Univ. Press, 1986.

[7] M. V. Berry and J. P. Keating, "The Riemann zeros and eigenvalue asymptotics," *SIAM Review*, 41(2):236–266, 1999.

[8] A. Connes, "Trace formula in noncommutative geometry and the zeros of the Riemann zeta function," *Selecta Mathematica*, 5:29–106, 1999.

[9] G. Sierra and P. K. Townsend, "The Riemann zeros and quantum chaos," *J. Phys. A: Math. Theor.*, 41:385202, 2008.

[10] J. P. Keating, "Random matrices and the Riemann zeros," *Contemp. Math.*, 290:57–73, 2001.